Optimum Co-Design for Spectrum Sharing between Matrix Completion Based MIMO Radars and a MIMO Communication System

Bo Li, *Student Member, IEEE*, Athina P. Petropulu, *Fellow, IEEE*, and Wade Trappe, *Fellow, IEEE*

这里主要强调了降低相互之间的干扰 EIP 有效干扰功率
MIMO-MC

***Abstract*—Spectrum sharing enables radar and communication systems to share the spectrum efficiently by minimizing mutual interference. Recently proposed multiple-input multiple-output radars based on sparse sensing and matrix completion (MIMO-MC), in addition to reducing communication bandwidth and power as compared with MIMO radars, offer a significant advantage for spectrum sharing. The advantage stems from the way the sampling scheme at the radar receivers modulates the interference channel from the communication system transmitters, rendering it symbol dependent and reducing its row space. This makes it easier for the communication system to design its waveforms in an adaptive fashion so that it minimizes the interference to the radar subject to meeting rate and power constraints. Two methods are proposed. First, based on the knowledge of the radar sampling scheme, the communication system transmit covariance matrix is designed to minimize the effective interference power (EIP) at the radar receiver, while maintaining certain average capacity and transmit power for the communication system. Second, a joint design of the communication transmit covariance matrix and the MIMO-MC radar sampling scheme is proposed, which achieves even further EIP reduction.**

稀疏传感 使，成为 给予 基本原理，根本 坚定，决心 探索的，寻根究底 获得 融合 选取，抽样

***Index Terms*—Collocated MIMO radar, matrix completion, spectrum sharing.**

MC

I. Introduction

THE operating frequency bands of communication and radar systems often overlap, causing one system to exert interference to the other. For example, the high UHF radar systems overlap with GSM communication systems, and the S-band radar systems partially overlap with Long Term Evolution (LTE) and WiMax systems [2]–[5]. Spectrum sharing is an emerging technology that can be applied to enable radar and communication systems to share the spectrum efficiently by minimizing mutual interference [4]–[14].

Manuscript received October 29, 2015; revised March 11, 2016; accepted May 07, 2016. Date of publication May 17, 2016; date of current version July 22, 2016. The associate editor coordinating the review of this manuscript and approving it for publication was Prof. Amir Asif. This work was supported by NSF under Grant ECCS-1408437. Parts of this work have been presented at the IEEE International Conference on Acoustics, Speech, and Signal Processing (ICASSP) 2015.

B. Li and A. P. Petropulu are with Department of Electrical and Computer Engineering, Rutgers, The State University of New Jersey, Piscataway NJ 08854 USA (e-mail: paul.bo.li@rutgers.edu; athinap@rutgers.edu).

W. Trappe is with the Department of Electrical and Computer Engineering, Rutgers University, Piscataway, NJ 08854 USA, and also with WINLAB, Rutgers University, North Brunswick, NJ 08901 USA (e-mail: trappe@winlab.rutgers.edu).

Color versions of one or more of the figures in this paper are available online at http://ieeexplore.ieee.org.

Digital Object Identifier 10.1109/TSP.2016.2569479

In this paper we study spectrum sharing between a special class of collocated MIMO radars and a MIMO communication system. The rationale behind considering a MIMO-type radar system is the high resolution which such systems can achieve with a relatively small number of transmit (TX) and receive (RX) antennas [15]–[18]. A MIMO radar system lends itself to a networked implementation, which is very desirable in both military and civilian applications. A networked radar is a configuration of TX and RX antennas. The TX antennas transmit probing waveforms, and target information is extracted by jointly processing the measurements of all RX antennas. This processing can be done at a fusion center, i.e., a network node endowed with more computational power than the rest of the nodes. Reliable surveillance requires collection, communication and fusion of vast amounts of data from various antennas. This is a power and bandwidth consuming task, which can be especially taxing in scenarios in which the antennas are on battery operated devices and are connected to the fusion center via a wireless link. Recently, MIMO radars using compressive sensing (MIMO-CS) [19]–[22], and MIMO radars via matrix completion (MIMO-MC) [23]–[26] have been proposed to save power and bandwidth on the link between the receivers and the fusion center, thus facilitating the network implementation of MIMO radars. MIMO-MC radars transmit orthogonal waveforms from their multiple TX antennas. Each RX antenna samples the target returns in a pseudo-random sub-Nyquist fashion and forwards the samples to the fusion center, along with the seed of the random sampling sequence. By collecting the samples of all RX antennas, and based on knowledge of each antenna's sampling scheme, the fusion center constructs a matrix, refereed to as the data matrix (see [24] Scheme I), in which only the entries corresponding to sampled times contain non-zero values. Subsequently, the missing entries, corresponding to non-sampled times, are provably recovered via MC techniques. In MIMO-MC radars the interference is confined to the sampled entries of the data matrix, while after matrix completion the target echo power is preserved. Unlike MIMO-CS, MIMO-MC does not require discretization of the target space, thus does not suffer from grid mismatch issues [27].

伪随机 离散化 网格不匹配问题

Spectrum sharing between a MIMO radar and a communication system has been considered in [5]–[9], where the radar interference is eliminated by projecting the radar waveforms onto the null space of the interference channel between the MIMO radar transmitters and the communication system. In [10], a radar receive filter was proposed to mitigate the interference from the communication systems. However, null space projection-type

减轻

or spatial filtering-type techniques might miss targets aligned with the interference channel. In general, the existing literature on MIMO radar-communication systems spectrum sharing addresses interference mitigation for either solely the communication system [5]–[9] or solely the radar [10]. While joint design of traditional radar and communication systems for spectrum sharing has been considered in [4], [13], [14], co-design of MIMO radar and MIMO communication systems for spectrum sharing has not been addressed before, with the exception of our preliminary results in [1], [28]. In practice, however, the two systems are often aware of the existence of each other, and they could share information, which could be exploited for co-design. Recent developments in cognitive radios [29] and cognitive radars [30] could provide the tools for information sharing and channel feedback, thus facilitating the cooperation between radar and communication systems.

Motivated by the cooperative methods in cognitive radio networks [31]–[33], we propose ways via which a MIMO-MC radar and a MIMO communication system, in a cooperative fashion, negotiate spectrum use in order to mitigate mutual interference. In addition to reducing communication bandwidth and power, MIMO-MC radars offer a significant advantage for spectrum sharing. The advantage stems from the way the sampling scheme at the radar receivers modulates the interference channel from the communication system transmitters, rendering it symbol dependent and reducing its row space. This makes it easier for the communication system to design its waveforms in an adaptive fashion to minimize its interference to the radar subject to meeting rate and power constraints. Two methods are proposed. The first method is a cooperative design; for a fixed radar sampling scheme, which is known to the communication system, the communication system optimally selects its precoding matrix to minimize the interference to the radar. The second method is a joint design, whereby the radar sampling scheme as well as the communication system precoding matrix are optimally selected to minimize the interference to the radar. For the first method, an efficient algorithm for solving the corresponding optimization problem is proposed based on the Lagrangian dual decomposition (see Algorithm 1). For the second method, alternating optimization is employed to solve the corresponding optimization problem. The candidate sampling scheme needs to be such that the resulting data matrix can be completed. Recent work [34] showed that for matrix completion, the sampling locations should correspond to a binary matrix with large spectral gap. Since the spectral gap of a matrix is not affected by column and row permutations, we propose to search for the optimum sampling matrix among matrices which are row and column permutations of an initial sampling matrix with large spectral gap.

The paper is organized as follows. Section III introduces the signal model when the MIMO-MC radar and communication systems coexist. The problem of a MIMO communication system sharing the spectrum with a MIMO-MC radar system is studied in Section IV. Numerical results, discussions and conclusions are provided in Section V–Section VII.

Notation: $\mathcal{CN}(\boldsymbol{\mu}, \boldsymbol{\Sigma})$ denotes the circularly symmetric complex Gaussian distribution with mean $\boldsymbol{\mu}$ and covariance matrix $\boldsymbol{\Sigma}$. $|\cdot|$, $\mathrm{Tr}(\cdot)$, $\|\cdot\|_*$ and $\|\cdot\|_F$ denote the matrix determinant, trace, nuclear norm and Frobenius norm, respectively. The set $\mathbb{N}_L^+$ is defined as $\{1, \ldots, L\}$. $\mathcal{N}(\mathbf{A})$ and $\mathcal{R}(\mathbf{A})$ denote the null and row spaces of matrix $\mathbf{A}$, respectively. $\mathbf{A}_{i\cdot}$ and $\mathbf{A}_{\cdot j}$ respectively, denote the i-th row and j-th column of matrix $\mathbf{A}$. $[\mathbf{A}]_{i,j}$ denotes the element on the i-th row and j-th column of matrix $\mathbf{A}$. x^+ is defined as $\max(0, x)$.

II. Background on MIMO-MC Radars

Consider a collocated MIMO radar system with $M_{t,R}$ TX antennas and $M_{r,R}$ RX antennas. The targets are in the far-field of the antennas and are assumed to fall in the same range bin. The radar operates in two phases; in the first phase the TX antennas transmit waveforms and the RX antennas receive target returns, while in the second phase, the RX antennas forward their measurements to a fusion center. In each pulse, the m-th, $m \in \mathbb{N}^+_{M_{t,R}}$, antenna transmits a coded waveform containing L symbols $\{s_m(1), \ldots, s_m(L)\}$ of duration T_R each. Each RX antenna samples the target returns every T_R seconds, i.e., samples each symbol exactly once. Following the model of [23]–[25], the data matrix at the fusion center can be formulated as

$$\mathbf{Y}_R = \gamma\rho\mathbf{D}\mathbf{S} + \mathbf{W}_R, \tag{1}$$

where the m-th row of $\mathbf{Y}_R \in \mathbb{C}^{M_{r,R} \times L}$ contains the L samples forwarded by the m-th antenna; γ and ρ respectively denote the path loss corresponding to the range bin of interest, and the radar transmit power; $\mathbf{D} \in \mathbb{C}^{M_{r,R} \times M_{t,R}}$ denotes the target response matrix, which depends on the target reflectivity, angle of arrival and target speed (details can be found in [24]); $\mathbf{S} = [\mathbf{s}(1), \ldots, \mathbf{s}(L)]$, with $\mathbf{s}(l) = [s_1(l), \ldots, s_{M_{t,R}}(l)]^T$ being the l-th snapshot across the transmit antennas. The transmit waveforms are assumed to be orthogonal, i.e., it holds that $\mathbf{S}\mathbf{S}^H = \mathbf{I}$ [24]; $\mathbf{W}_R$ denotes additive noise. After matched filtering at the fusion center, target estimation can be performed based on $\mathbf{Y}_R$ via standard array processing schemes [35].

If the number of targets is smaller than $M_{r,R}$ and L, matrix $\mathbf{D}\mathbf{S}$ is low-rank and can be provably recovered based on a subset of its entries [24], [26]. This observation gave rise to MIMO-MC radars [23]–[26], where each RX antenna sub-samples the target returns and forwards the samples to the fusion center. The sampling scheme could be a pseudo-random sequence of integers in $[1, L]$, with the fusion center knowing the random seed of each RX antenna. In MIMO-MC radars, the partially filled data matrix at the fusion center can be mathematically expressed as follows (see [24] Scheme I)

$$\boldsymbol{\Omega} \circ \mathbf{Y}_R = \boldsymbol{\Omega} \circ (\gamma\rho\mathbf{D}\mathbf{S} + \mathbf{W}_R), \tag{2}$$

where $\circ$ denotes Hadamard product and $\boldsymbol{\Omega}$ is a matrix containing 0's and 1's; the 1's in the m-th row correspond to the sampled symbols of the m-th RX antenna. The sub-sampling rate, p, equals $\|\boldsymbol{\Omega}\|_0/(LM_{r,R})$. When $p = 1$, the $\boldsymbol{\Omega}$ matrix is filled with 1's, and the MIMO-MC radar is identical to the traditional MIMO radar. At the fusion center, the completion of $\gamma\rho\mathbf{D}\mathbf{S}$ is

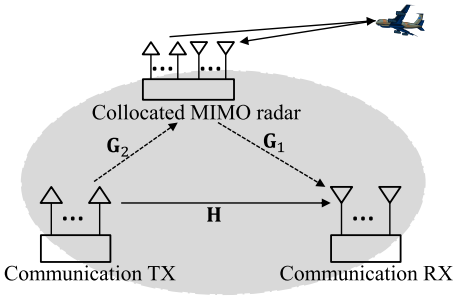

Fig. 1. MIMO communication system sharing spectrum with a colocated MIMO radar system.

formulated as the following problem [36]

$$\min_{\mathbf{M}} \| \mathbf{M} \|_* \quad \text{s.t.} \| \mathbf{\Omega} \circ \mathbf{M} - \mathbf{\Omega} \circ \mathbf{Y}_R \|_F \leq \delta, \tag{3}$$

where $\delta > 0$ is a parameter related to the noise over the sampled noise matrix entries, i.e., $\mathbf{\Omega} \circ \mathbf{W}_R$. On denoting by $\widehat{\mathbf{M}}$ the solution of (3), the recovery error $\| \widehat{\mathbf{M}} - \gamma\rho\mathbf{DS} \|_F$ is determined by the noise power in $\mathbf{\Omega} \circ \mathbf{W}_R$, i.e., the noise enters only through the sampled entries of the data matrix. It is important to note that, assuming that the reconstruction error is small, the reconstructed $\widehat{\mathbf{M}}$ has the same received target echo power as $\gamma\rho\mathbf{DS}$ of (1).

Early studies on matrix completion theory suggested that the low-rank matrix reconstruction requires that the entries are sampled uniformly at random. However, recent works [34] showed that non-uniform sampling would still work, as long as the sampling matrix has large spectral gap (i.e., large gap between the largest and second largest singular values).

奇数的，单数的

III. System Model 系统模型

Consider a MIMO communication system which coexists with a MIMO-MC radar system as shown in Fig. 1, sharing the same carrier frequency. The MIMO-MC radar operates in two phases, i.e., in Phase 1 the RX antennas obtain measurements of the target returns, and in Phase 2, the RX antennas forward the obtained samples to a fusion center. The communication system interferes with the radar system during both phases. In the following, we will address spectrum sharing during the first phase only. The interference during the second phase can be viewed as the interference between two communication systems; addressing this problem has been covered in the literature [31], [32].

Suppose that the two systems have the same symbol rate and are synchronized in terms of sampling times (see Section V for the mismatched case). We do not assume perfect carrier phase synchronization between the two systems. The data matrix at the radar fusion center, and the received matrix at the communication RX antennas during L symbol durations can be respectively expressed as

Radar fusion center:

$$\mathbf{\Omega} \circ \mathbf{Y}_R = \underbrace{\mathbf{\Omega} \circ (\gamma\rho\mathbf{DS})}_{\text{signal}} + \underbrace{\mathbf{\Omega} \circ (\mathbf{G}_2\mathbf{X}\mathbf{\Lambda}_2)}_{\text{interference}} + \underbrace{\mathbf{\Omega} \circ \mathbf{W}_R}_{\text{noise}}, \tag{4a}$$

Communication receiver:

$$\mathbf{Y}_C = \underbrace{\mathbf{HX}}_{\text{signal}} + \underbrace{\rho\mathbf{G}_1\mathbf{S}\mathbf{\Lambda}_1}_{\text{interference}} + \underbrace{\mathbf{W}_C}_{\text{noise}}, \tag{4b}$$

where

1) $\mathbf{Y}_R$, ρ, $\mathbf{D}$, $\mathbf{S}$, $\mathbf{W}_R$, and $\mathbf{\Omega}$ are defined in Section II.
2) $\mathbf{X} \triangleq [\mathbf{x}(1), \ldots, \mathbf{x}(L)]$; $\mathbf{x}(l) \in \mathbb{C}^{M_{t,C} \times 1}$ denotes the transmit vector by the communication TX antennas during the l-th symbol duration. The rows of $\mathbf{X}$ are codewords from the code-book of the communication system.
3) $\mathbf{W}_C$ and $\mathbf{W}_R$ denote the additive noise; their elements are assumed to be independent identically distributed as $\mathcal{CN}(0, \sigma_C^2)$ and $\mathcal{CN}(0, \sigma_R^2)$, respectively.

加性噪声

4) $\mathbf{H} \in \mathbb{C}^{M_{r,C} \times M_{t,C}}$ denotes the communication channel, where $M_{r,C}$ and $M_{t,C}$ denote respectively the number of RX and TX antennas of the communication system; $\mathbf{G}_1 \in \mathbb{C}^{M_{r,C} \times M_{t,R}}$ denotes the interference channel from the radar TX antennas to the communication system RX antennas; $\mathbf{G}_2 \in \mathbb{C}^{M_{r,R} \times M_{t,C}}$ denotes the interference channel from the communication TX antennas to the radar RX antennas. All channels are assumed to be flat fading and remain the same over L symbol intervals [5], [6], [8], [31].
5) $\mathbf{\Lambda}_1$ and $\mathbf{\Lambda}_2$ are diagonal matrices. The l-th diagonal entry of $\mathbf{\Lambda}_1$, i.e., $e^{j\alpha_{1l}}$, denotes the random phase offset between the MIMO-MC radar carrier and the communication receiver reference carrier at the l-th sampling time. The l-th diagonal entry of $\mathbf{\Lambda}_2$, i.e., $e^{j\alpha_{2l}}$, denotes the random phase offset between the communication transmitter carrier and the MIMO-MC radar reference carrier at the l-th sampling time. The phase offsets arise due to random phase jitter of the radar oscillator and the oscillator at the communication receiver Phase-Locked Loops. In the literature [37]–[39], the phase jitter of oscillator $\alpha(t)$ is modeled as a zero-mean Gaussian process. In this paper, we model $\{\alpha_{1l}\}_{l=1}^{L}$ as a sequence of zero-mean Gaussian random variables with variance σ_α^2. Modern CMOS oscillators exhibit very low phase noise, e.g., -94 dB below the carrier power per Hz (i.e., -94 dBc/Hz) at an offset of $2\pi \times 1$ MHz, which yields phase jitter variance $\sigma_\alpha^2 \approx 2.5 \times 10^{-3}$ [40].

对角矩阵

The following assumptions are made: 假设

1) *About the synchronization of sampling times*—We assume that the radar receivers and the communication system sample in a time synchronous manner. Although this assumption is later relaxed in Section V, we next provide an example of radar and communication parameter settings suggesting that the aforementioned assumption is applicable in real world systems. The typical range resolution for an S-band search and acquisition radar is between 100 m and 600 m [41], [42]. Thus, for range resolution of $cT_b/2 = 300$ m, where $c = 3 \times 10^8$ m/s denotes the speed of light, the radar sub-pulse duration is $T_b = 2$ μs. In order to have identical symbol rate for two systems, the communication symbol duration should be 2 μs, which corresponds to signal bandwidth of 0.5 MHz. This symbol interval value falls in the typical range of symbol interval values in LTE systems [43].

同步

前述的

2) *About channel fading*—We assume that $\mathbf{H}$, $\mathbf{G}_1$ and $\mathbf{G}_2$ are flat fading, which is valid when the channel coherence bandwidth is larger than the signal bandwidth [44]–[46], i.e., when the transmitted signals are narrowband. Consider the symbol interval value 2 μs and signal bandwidth 0.5 MHz given above. In a LTE macro-cell, the coherence bandwidth is in the order of 1 MHz [43], [47]. The typical values of LTE channel coherence bandwidth are much larger than the signal bandwidth of 0.5 MHz, thus making the flat fading channel assumption valid. Since the radar and communication systems use the same carrier and signal bandwidth, the flat fading assumption is valid for all $\mathbf{H}$, $\mathbf{G}_1$ and $\mathbf{G}_2$. In the radar-communication system coexistence literature [5]–[9], the flat fading assumption is quite typical. If the narrowband assumption is not valid then perhaps one could consider an OFDM scenario, where the flat fading model would apply on each carrier [13], [14].

3) *About channel information feedback*—The channels $\mathbf{H}$ and $\mathbf{G}_2$ are also assumed to be perfectly known at the communication TX antennas. In practice, such channel information can be obtained at the radar RX antennas through the transmission of pilot signals [5], [48]. Viewing the radar system as the primary user of a cognitive radio system and the MIMO communication system as the secondary user, techniques similar to those of [31]–[33], [49] can be used to estimate and feed back the channel information between the primary and secondary systems.

Let $\mathbf{S}_{\text{obs}} \triangleq \rho\mathbf{G}_1\mathbf{S}$ be the radar interference as viewed by the communication system. This can be obtained during times that the communication system does not transmit. Since the radar transmission power ρ is very high, $\rho\mathbf{G}_1\mathbf{S}$ can be estimated with high accuracy. Based on $\mathbf{S}_{\text{obs}}$, the communication receivers can eliminate some of the interference via direct subtraction. However, due to the high power of the radar [3] and the unknown phase offset, there will always be residual interference, i.e.,

$$\rho\mathbf{G}_1\mathbf{S}\left(\mathbf{\Lambda}_1 - \mathbf{I}\right) \approx \rho\mathbf{G}_1\mathbf{S}\mathbf{\Lambda}_\alpha \equiv \mathbf{S}_{\text{obs}}\mathbf{\Lambda}_\alpha, \tag{5}$$

where $\mathbf{\Lambda}_\alpha = \text{diag}(j\alpha_{11}, \ldots, j\alpha_{1L})$, and the approximation is based on the fact that $\{\alpha_{1l}\}_{l=1}^{L}$ are small. In the above, we assume that the radar waveforms have not changed between the time the interference is estimated and used in (5). The signal at the communication receiver after interference cancellation equals

$$\widetilde{\mathbf{Y}}_C = \mathbf{H}\mathbf{X} + \mathbf{S}_{\text{obs}}\mathbf{\Lambda}_\alpha + \mathbf{W}_C. \tag{6}$$

This residual interference is not circularly symmetric, and thus the communication channel capacity is achieved by non-circularly symmetric Gaussian codewords, whose covariance and complementary covariance matrix would need to be designed simultaneously [50]. Here, we consider circularly symmetric complex Gaussian codewords $\mathbf{x}(l) \sim \mathcal{CN}(0, \mathbf{R}_{xl})$, which achieve a lower bound of the channel capacity [50], [51]. This reduces the complexity of the design since we only need to design the transmit covariance matrix $\mathbf{R}_{xl}$.

Unless special measures are taken, the interference from the radar transmissions, i.e., $\mathbf{S}_{\text{obs}}\mathbf{\Lambda}_\alpha$, will reduce the communication system capacity, and the interference from the communication system transmission, i.e., $\mathbf{\Omega} \circ (\mathbf{G}_2\mathbf{X}\mathbf{\Lambda}_2)$ will degrade the completion of the data matrix and as a result the target detection/estimation. The application of traditional spatial filtering on $\mathbf{\Omega} \circ \mathbf{Y}_\mathbf{R}$ for eliminating the communication system interference is not straightforward and to the best of our knowledge has not been previously addressed. For the case with complete samples, the optimal detector to maximize the SINR is matched filtering following a whitening filter. However, in the case of partially sampled $\mathbf{Y}_\mathbf{R}$, i.e., $\mathbf{\Omega} \circ \mathbf{Y}_\mathbf{R}$, $\mathbf{S}$ cannot be fully matched due to the sub-sampling operator. Also, the interference plus noise at the whitening filter output would not be white anymore. Further, note that the recovery of $\gamma\rho\mathbf{DS}$ via matrix completion in (3) is based on $(\mathbf{\Omega} \circ \mathbf{Y}_R)$. Even if we somehow find the spatial filter $\mathbf{W}$ that maximizes the SINR, the filter output $\mathbf{W}(\mathbf{\Omega} \circ \mathbf{Y}_R)$ cannot be used by the matrix completion formulation in (3), which follows the formulation in the MIMO-MC radar [23]–[26] and general matrix completion literature [36]. The extension of the matrix completion working with the additional filtering matrix is out the scope of this paper. Of course, one could apply filtering on the recovered data matrix $\mathbf{DS}$ as post processing. However, such post-filtering would first need the matrix completion to be successful.

The approach that we propose here for addressing the radar and comm systems interference is a design for the communication TX signals, or a co-design of the communication TX signals and the radar sub-sampling scheme, so that we minimize the interference at the radar RX antennas for successful matrix completion, while satisfying certain communication system rate requirements.

IV. Spectrum Sharing Between MIMO-MC Radar and a MIMO Communication System

First, let us provide expressions for the communication TX power and channel capacity, and the interference power at the MIMO-MC radar receiver. The total transmit power of the communication TX antennas equals

$$\mathbb{E}\left\{\text{Tr}\left(\mathbf{X}\mathbf{X}^H\right)\right\} = \mathbb{E}\left\{\text{Tr}\left(\sum_{l=1}^{L}\mathbf{x}\left(l\right)\mathbf{x}^H\left(l\right)\right)\right\} = \sum_{l=1}^{L}\text{Tr}\left(\mathbf{R}_{xl}\right),$$

where $\mathbf{R}_{xl} \triangleq \mathbb{E}\{\mathbf{x}(l)\mathbf{x}^H(l)\}$.

Due to the sampling performed at the MIMO-MC radar receiver, the *effective interference power* (EIP) at the radar RX nodes can be expressed as:

$$\begin{aligned}
\text{EIP} &\triangleq \mathbb{E}\left\{\text{Tr}\left(\left(\mathbf{\Omega} \circ (\mathbf{G}_2\mathbf{X}\mathbf{\Lambda}_2\right)\left(\mathbf{\Omega} \circ (\mathbf{G}_2\mathbf{X}\mathbf{\Lambda}_2)\right)^H\right)\right\} \\
&= \mathbb{E}\left\{\text{Tr}\left([\mathbf{G}_{21}\mathbf{x}\left(1\right)\ldots\mathbf{G}_{2L}\mathbf{x}\left(L\right)]\mathbf{\Lambda}_2\mathbf{\Lambda}_2^H\right.\right. \\
&\quad \left.\left.\times\left[\mathbf{G}_{21}\mathbf{x}\left(1\right)\ldots\mathbf{G}_{2L}\mathbf{x}\left(L\right)\right]^H\right)\right\} \\
&= \mathbb{E}\left\{\text{Tr}\left(\sum_{l=1}^{L}\mathbf{G}_{2l}\mathbf{x}\left(l\right)\mathbf{x}^H\left(l\right)\mathbf{G}_{2l}^H]\right)\right\} \\
&= \sum_{l=1}^{L}\text{Tr}\left(\mathbf{G}_{2l}\mathbf{R}_{xl}\mathbf{G}_{2l}^H\right) = \sum_{l=1}^{L}\text{Tr}\left(\mathbf{\Delta}_l\mathbf{G}_2\mathbf{R}_{xl}\mathbf{G}_2^H\right),
\end{aligned} \tag{7}$$

where $\mathbf{G}_{2l} \triangleq \mathbf{\Delta}_l \mathbf{G}_2$, with $\mathbf{\Delta}_l = \text{diag}(\mathbf{\Omega}_{\cdot l})$. We note that the EIP at sampling time l contains the interference corresponding only to 1's in $\mathbf{\Omega}_{\cdot l}$. Thus, the effective interference channel during the l-th symbol duration is $\mathbf{G}_{2l}$. In the following, the EIP is used as the figure of merit for MIMO-MC radars as it affects the performance of matrix completion and further target estimation (see simulation results in Section VI.A). Before matrix completion and any target estimation, the EIP should be minimized. From another perspective, the EIP is a reasonable surrogate of the radar SINR, which is widely used as figure of merit in the literature [52], [53], as in this paper we do not assume any prior information on target parameters.

In the coexistence model of (4a) and (6), both the effective interference channel $\mathbf{G}_{2l}$, and the interference covariance matrix at the communication receiver, i.e., $\mathbf{R}_{\text{int}l} \triangleq \sigma_\alpha^2 \mathbf{S}_{\text{obs}}(l)\mathbf{S}_{\text{obs}}^H(l)$, vary between sampling times. Thus, the optimum scheme for the communication transmitter would be adaptive/dynamic transmission. A symbol dependent covariance matrix, i.e., $\mathbf{R}_{xl}$, would need to be designed for each symbol duration in order to match the variation of $\mathbf{G}_{2l}$ and $\mathbf{R}_{\text{int}l}$.

The channel $\mathbf{G}_{2l}$ can be equivalently viewed as a fast fading channel with perfect channel state information at both the transmitter and receiver [45], [54]. Similar to the definition of ergodic capacity [54], the achieved capacity is the average over L symbols, i.e.,

$$\text{C}_{\text{avg}}\left(\{\mathbf{R}_{xl}\}\right) \triangleq \frac{1}{L}\sum_{l=1}^{L} \log_2 \left|\mathbf{I} + \mathbf{R}_{wl}^{-1}\mathbf{H}\mathbf{R}_{xl}\mathbf{H}^H\right|, \quad (8)$$

where $\{\mathbf{R}_{xl}\}$ denotes the set of all $\mathbf{R}_{xl}$'s and $\mathbf{R}_{wl} \triangleq \mathbf{R}_{\text{int}l} + \sigma_C^2\mathbf{I}$ for all $l \in \mathbb{N}_L^+$.

The adaptive transmission could be implemented using the V-BLAST transmitter architecture ([45], Chapter 7), where the precoding matrix for symbol index l is set to $\mathbf{R}_{xl}^{1/2}$. This idea is also used in the transceiver architecture for achieving the capacity of a fast fading MIMO channel with full channel state information ([45], Chapter 8.2.3), and is also discussed in ([46], Chapter 9). The adaptive transmission in response to highly mobile, fast fading channels requires the transmitter to vary the rate, power and even the coding strategy. The main bottleneck of the system is not due to the complexity of designing and implementing the variable transmission parameters, but rather due to the feedback delay of the fast fading channel. In our paper, the latter issue is not relevant because the channel variations are introduced by the MC technique and radar waveforms, which are available at the communication transmitter.

In this section, spectrum sharing between the communication system and the MIMO-MC radar is achieved by minimizing the interference power at the MIMO-MC radar RX node, while satisfying the communication rate and TX power constraints of the communication system. The design variables are the communication TX covariance matrices and/or the radar sub-sampling scheme. In the following we will consider two approaches, namely a cooperative and a joint design approach.

A. Cooperative Spectrum Sharing

In the *cooperative approach*, the MIMO-MC radar shares its sampling scheme $\mathbf{\Omega}$ with the communication system. The spectrum sharing problem can be formulated as

$$(\mathbf{P}_1) \quad \min_{\{\mathbf{R}_{xl}\}\succeq 0} \text{EIP}\left(\{\mathbf{R}_{xl}\}\right) \text{ s.t. } \sum_{l=1}^{L} \text{Tr}\left(\mathbf{R}_{xl}\right) \le P_t \quad (9a)$$

$$\text{C}_{\text{avg}}\left(\{\mathbf{R}_{xl}\}\right) \ge C, \quad (9b)$$

where the constraint of (9a) restricts the total transmit power at the communication TX antennas to be no larger than P_t. The constraint of (9b) restricts the communication average capacity during L symbol durations to be at least C, in order to provide reliable communication and avoid service outage. $\{\mathbf{R}_{xl}\} \succeq 0$ imposes the positive semi-definiteness on the solution.

Problem $(\mathbf{P}_1)$ is convex and involves multiple matrix variables, the joint optimization with respect to which requires high computational complexity. Fortunately, we observe that both the objective and constraints are separable functions of $\{\mathbf{R}_{xl}\}$. An efficient algorithm for solving the above problem can be implemented based on the Lagrangian dual decomposition [55] as follows.

1) An Efficient Algorithm Based on Dual Decomposition: The Lagrangian of $(\mathbf{P}_1)$ can be written as

$$\mathcal{L}\left(\{\mathbf{R}_{xl}\}, \lambda_1, \lambda_2\right) = \text{EIP}\left(\{\mathbf{R}_{xl}\}\right) + \lambda_2\left(C - \text{C}_{\text{avg}}\left(\{\mathbf{R}_{xl}\}\right)\right) + \lambda_1\left(\sum_{l=1}^{L}\text{Tr}\left(\mathbf{R}_{xl}\right) - P_t\right),$$

where $\lambda_1 \ge 0$ is the dual variable associated with the transmit power constraint, and $\lambda_2 \ge 0$ is the dual variable associated with the average capacity constraint. The dual problem of $(\mathbf{P}_1)$ is

$$(\mathbf{P}_1 - \mathbf{D}) \quad \max_{\lambda_1,\lambda_2\ge 0} g\left(\lambda_1, \lambda_2\right),$$

where $g(\lambda_1, \lambda_2)$ is the dual function defined as

$$g\left(\lambda_1, \lambda_2\right) = \inf_{\{\mathbf{R}_{xl}\}\succeq 0} \mathcal{L}\left(\{\mathbf{R}_{xl}\}, \lambda_1, \lambda_2\right).$$

The domain of the dual function, i.e., $\text{dom}\, g$, is $\lambda_1, \lambda_2 \ge 0$ such that $g(\lambda_1, \lambda_2) > -\infty$. It is also called dual feasible if $(\lambda_1, \lambda_2) \in \text{dom}\, g$. It is interesting to note that $g(\lambda_1, \lambda_2)$ can be obtained by solving L independent subproblems, each of which can be written as follows

$$(\mathbf{P}_1\text{-sub}) \quad \min_{\mathbf{R}_{xl}\succeq 0} \text{Tr}\left(\left(\mathbf{G}_2^H\mathbf{\Delta}_l\mathbf{G}_2 + \lambda_1\mathbf{I}\right)\mathbf{R}_{xl}\right) - \lambda_2 \log_2\left|\mathbf{I} + \mathbf{R}_{wl}^{-1}\mathbf{H}\mathbf{R}_{xl}\mathbf{H}^H\right|. \quad (10)$$

Before giving the solution of $(\mathbf{P}_1\text{-sub})$, let us first state some observations.

Observation 1: The average capacity constraint should be active at the optimal point. This means that the achieved capacity is always C and $\lambda_2 > 0$. To show this, let us assume that the optimal point $\{\mathbf{R}_{xl}^*\}$ achieves $\text{C}_{\text{avg}}(\{\mathbf{R}_{xl}^*\}) > C$. Then we can always shrink $\{\mathbf{R}_{xl}^*\}$ until the average capacity reduces to C, which would also reduce the objective. Thus, we end up with a

Algorithm 1: Cooperative Spectrum Sharing $(\mathbf{P}_1)$.

1: **Input:** $\mathbf{H}, \mathbf{G}_1, \mathbf{G}_2, \mathbf{\Omega}, P_t, C, \sigma_C^2$
2: **Initialization:** $\lambda_1 \geq 0, \lambda_2 \geq 0$
3: **repeat**
4: Calculate $\mathbf{R}_{xl}^*(\lambda_1, \lambda_2)$ according to (11) with the given λ_1 and λ_2;
5: Compute the subgradient of $g(\lambda_1, \lambda_2)$ as $\sum_{l=1}^{L} \mathrm{Tr}(\mathbf{R}_{xl}^*(\lambda_1, \lambda_2)) - P_t$ and $C - \mathrm{C}_{\mathrm{avg}}(\{\mathbf{R}_{xl}^*(\lambda_1, \lambda_2)\})$ respectively for λ_1 and λ_2;
6: Update λ_1 and λ_2 accordingly based on the ellipsoid method [56];
7: **until** λ_1 and λ_2 converge to a prescribed accuracy.
8: **Output:** $\mathbf{R}_{xl}^* = \mathbf{R}_{xl}^*(\lambda_1, \lambda_2)$

contradiction. By complementary slackness, the corresponding dual variable is positive, i.e., $\lambda_2 > 0$.

Observation 2: $(\mathbf{G}_2^H \mathbf{\Delta}_l \mathbf{G}_2 + \lambda_1 \mathbf{I})$ is positive definite for all $l \in \mathbb{N}_L^+$. This can be shown by contradiction. Suppose that there exists l such that $\mathbf{G}_2^H \mathbf{\Delta}_l \mathbf{G}_2 + \lambda_1 \mathbf{I}$ is singular. Then it must hold that $\mathbf{G}_2^H \mathbf{\Delta}_l \mathbf{G}_2$ is singular and $\lambda_1 = 0$. Therefore, we can always find a nonzero vector $\mathbf{v}$ lying in the null space of $\mathbf{G}_2^H \mathbf{\Delta}_l \mathbf{G}_2$. At the same time, it holds that $\mathbf{R}_{wl}^{-1/2} \mathbf{H} \mathbf{v} \neq 0$ with very high probability, because $\mathbf{H}$ is a realization of the random channel. If we choose $\mathbf{R}_{xl} = \alpha \mathbf{v}\mathbf{v}^H$ and $\alpha \to \infty$, the Lagrangian $\mathcal{L}(\{\mathbf{R}_{xl}\}, 0, \lambda_2)$ will be unbounded from below, which indicates that $\lambda_1 = 0$ is not dual feasible. This means that λ_1 is strictly larger than 0 if $\mathbf{G}_2^H \mathbf{\Delta}_l \mathbf{G}_2$ is singular for any l. Thus, the claim is proven.

Based on the above observations, we have the following lemma.

Lemma 1 ([32], [33]): For given feasible dual variables $\lambda_1, \lambda_2 \geq 0$, the optimal solution of $(\mathbf{P}_1\text{-sub})$ is given by

$$\mathbf{R}_{xl}^* (\lambda_1, \lambda_2) = \mathbf{\Phi}_l^{-1/2} \mathbf{U}_l \mathbf{\Sigma}_l \mathbf{U}_l^H \mathbf{\Phi}_l^{-1/2}, \tag{11}$$

where $\mathbf{\Phi}_l \triangleq \mathbf{G}_2^H \mathbf{\Delta}_l \mathbf{G}_2 + \lambda_1 \mathbf{I}$; $\mathbf{U}_l$ is the right singular matrix of $\widetilde{\mathbf{H}}_l \triangleq \mathbf{R}_{wl}^{-1/2} \mathbf{H} \mathbf{\Phi}_l^{-1/2}$; $\mathbf{\Sigma}_l = \mathrm{diag}(\beta_{l1}, \ldots, \beta_{lr})$ with $\beta_{li} = (\lambda_2 - 1/\sigma_{li}^2)^+$, r and $\sigma_{li}, i = 1, \ldots, r$, respectively being the rank and the positive singular vales of $\widetilde{\mathbf{H}}_l$. It also holds that

$$\log_2 \left| \mathbf{I} + \mathbf{R}_{wl}^{-1} \mathbf{H} \mathbf{R}_{xl}^* \mathbf{H}^H \right| = \sum_{i=1}^{r} \left(\log \left(\lambda_2 \sigma_{li}^2 \right) \right)^+. \tag{12}$$

Based on Lemma 1, the solution of $(\mathbf{P}_1)$ can be obtained by finding the optimal dual variables λ_1^*, λ_2^*. The cooperative spectrum sharing problem $(\mathbf{P}_1)$ can be solved via the procedure outlined in Algorithm 1. The convergence of Algorithm 1 is guaranteed by the convergence of the ellipsoid method [56].

Based on Lemma 1, the coexistence model can be equivalently viewed as a fast fading MIMO channel $\widetilde{\mathbf{H}}_l$. The covariance of the waveforms transmitted on $\widetilde{\mathbf{H}}_l$ is $\widetilde{\mathbf{R}}_{xl} \triangleq \mathbf{\Phi}_l^{1/2} \mathbf{R}_{xl} \mathbf{\Phi}_l^{1/2}$. It is well-known that the optimum $\widetilde{\mathbf{R}}_{xl}$ equals $\mathbf{U}_l \mathbf{\Sigma}_l \mathbf{U}_l^H$ with power allocation obtained by the water-filling algorithm [54]. The achieved capacity is the average over all realization of the channel, i.e., $\{\widetilde{\mathbf{H}}_l\}_{l=1}^{L}$. This justifies the definition of average capacity in (8). Lemma 1 shows that the communication transmitter will allocate more power to directions determined by the left singular vectors of $\mathbf{H}$ corresponding to larger eigenvalues and by the eigenvectors of $\mathbf{\Phi}_l$ corresponding to smaller eigenvalues. In other words, the communication will transmit more power in directions that convey larger signal at the communication receivers and smaller interferences to the MIMO-MC radars.

2) Spectrum Sharing Without Knowledge of the Radar's Sampling Scheme: If the MIMO-MC radar does not share $\mathbf{\Omega}$ with the communication system, the expression of EIP of (7) is also not available at the communication system. In this case, the communication system can design its covariance assuming that $\mathbf{\Omega}$ is full of 1's, i.e., for the worst case of interference

$$(\mathbf{P}_0) \quad \min_{\{\mathbf{R}_{xl}\} \succeq 0} \sum_{l=1}^{L} \mathrm{Tr} \left(\mathbf{G}_2 \mathbf{R}_{xl} \mathbf{G}_2^H \right)$$
$$\text{s.t.} \sum_{l=1}^{L} \mathrm{Tr} \left(\mathbf{R}_{xl} \right) \leq P_t, \mathrm{C}_{\mathrm{avg}} \left(\{\mathbf{R}_{xl}\} \right) \geq C. \tag{13}$$

The same design would hold for the case in which a traditional MIMO radar is used instead of a MIMO-MC radar. Problem $(\mathbf{P}_0)$ is also convex and has exactly the same constraints as $(\mathbf{P}_1)$. The efficient algorithm based on the dual decomposition technique in Algorithm 1 could also be applied to solve $(\mathbf{P}_0)$.

The following theorem compares the minimum EIP achieved by the cooperative approaches of $(\mathbf{P}_0)$ and $(\mathbf{P}_1)$ under the same communication constraints.

Theorem 1: For any P_t and C, the EIP achieved by the cooperative approaches of $(\mathbf{P}_1)$ is less or equal than that achieved by the approach of $(\mathbf{P}_0)$.

Proof: Let $\{\mathbf{R}_{xl}^{*0}\}$ and $\{\mathbf{R}_{xl}^{*1}\}$ denote the solution of $(\mathbf{P}_0)$ and $(\mathbf{P}_1)$, respectively. We know that $\{\mathbf{R}_{xl}^{*0}\}$ satisfies the constraints in $(\mathbf{P}_1)$, which means that $\{\mathbf{R}_{xl}^{*0}\}$ is a feasible point of $(\mathbf{P}_1)$. The optimal $\{\mathbf{R}_{xl}^{*1}\}$ achieves an objective value no larger than any feasible point, including $\{\mathbf{R}_{xl}^{*0}\}$. It holds that $\mathrm{EIP}(\{\mathbf{R}_{xl}^{*1}\}) \leq \mathrm{EIP}(\{\mathbf{R}_{xl}^{*0}\})$, which proves the claim. ■

There are certain scenarios in which $(\mathbf{P}_1)$ outperforms $(\mathbf{P}_0)$ significantly in terms of EIP. Let us denote by ϕ_1 the intersection of null space $\mathcal{N}(\mathbf{G}_{2l})$ and range space $\mathcal{R}(\mathbf{R}_{wl}^{1/2} \mathbf{H})$, and by ϕ_2 the intersection of null space $\mathcal{N}(\mathbf{G}_2)$ and range space $\mathcal{R}(\mathbf{R}_{wl}^{1/2} \mathbf{H})$. It holds that $\phi_2 \subseteq \phi_1$. Consider the case where ϕ_1 is nonempty while ϕ_2 is empty. This happens with high probability when $M_{r,R} \geq M_{t,C}$ but $pM_{r,R}$ is much smaller than $M_{t,C}$. Problem $(\mathbf{P}_1)$ will guide the communication system to focus its transmission power along the directions in ϕ_1 to satisfy both communication system constraints, while introducing zero EIP to the radar system. On the other hand, since ϕ_2 is empty, Problem $(\mathbf{P}_0)$ will guide the communication system transmit power along directions that introduce nonzero EIP. In other words, the sub-sampling procedure in the MIMO-MC radar essentially modulates the interference channel from the communication transmitter to the radar receiver by multiplying $\{\mathbf{\Delta}_l\}$. Compared to the original interference channel $\mathbf{G}_2$, the

dimension of the row space of modulated channel $\mathbf{G}_{2l}$ may be greatly reduced. The cooperative approach allows the communication system to optimally design the communication precoding matrices with respect to the effective interference channel $\mathbf{G}_{2l}$. Therefore, it is expected that the cooperative approach based on the knowledge of $\mathbf{\Omega}$, i.e., $(\mathbf{P}_1)$, introduces smaller EIP than its counterpart approach without knowledge of $\mathbf{\Omega}$, i.e., $(\mathbf{P}_0)$, does under the same the communication constraints.

B. Joint Communication and Radar System Design for Spectrum Sharing

In the above described spectrum sharing strategies, the MIMO-MC radar operates with a predetermined pseudo random sampling scheme. In this section, we consider a joint design of the communication system transmit covariance matrices and the MIMO-MC radar random sampling scheme, i.e., $\mathbf{\Omega}$. The candidate sampling scheme needs to ensure that the resulting data matrix can be completed. This means that $\mathbf{\Omega}$ is either a uniformly random sub-sampling matrix [36], or a matrix with a large spectral gap [34].

Recall that EIP $= \sum_{l=1}^{L} \mathrm{Tr}(\mathbf{\Delta}_l \mathbf{G}_2 \mathbf{R}_{xl} \mathbf{G}_2^H)$. The joint design scheme is formulated as

$$(\mathbf{P}_2) \quad \min_{\{\mathbf{R}_{xl}\} \succeq 0, \mathbf{\Omega}} \sum_{l=1}^{L} \mathrm{Tr}\left(\mathbf{\Delta}_l \mathbf{G}_2 \mathbf{R}_{xl} \mathbf{G}_2^H\right)$$
$$\text{s.t.} \sum_{l=1}^{L} \mathrm{Tr}\left(\mathbf{R}_{xl}\right) \le P_t, \mathrm{C}_{\text{avg}}\left(\{\mathbf{R}_{xl}\}\right) \ge C,$$
$$\mathbf{\Delta}_l = \mathrm{diag}\left(\mathbf{\Omega}_{\cdot l}\right), \mathbf{\Omega} \text{ is proper.}$$

The above problem is not convex. A solution can be obtained via alternating optimization. Let $(\{\mathbf{R}_{xl}^n\}, \mathbf{\Omega}^n)$ be the variables at the n-th iteration. We alternatively solve the following two problems:

$$\{\mathbf{R}_{xl}^n\} = \arg\min_{\{\mathbf{R}_{xl}\} \succeq 0} \sum_{l=1}^{L} \mathrm{Tr}\left(\mathbf{\Delta}_l^{n-1} \mathbf{G}_2 \mathbf{R}_{xl} \mathbf{G}_2^H\right),$$
$$\text{s.t.} \sum_{l=1}^{L} \mathrm{Tr}\left(\mathbf{R}_{xl}\right) \le P_t, \mathrm{C}_{\text{avg}}\left(\{\mathbf{R}_{xl}\}\right) \ge C, \quad (14a)$$

$$\mathbf{\Omega}^n = \arg\min_{\mathbf{\Omega}} \sum_{l=1}^{L} \mathrm{Tr}\left(\mathbf{\Delta}_l \mathbf{G}_2 \mathbf{R}_{xl}^n \mathbf{G}_2^H\right),$$
$$\text{s.t. } \mathbf{\Delta}_l = \mathrm{diag}\left(\mathbf{\Omega}_{\cdot l}\right), \mathbf{\Omega} \text{ is proper.} \quad (14b)$$

The problem of (14a) is convex and can be solved efficiently. By simple algebraic manipulation, the EIP can be reformulated as EIP $= \mathrm{Tr}(\mathbf{\Omega}^T \mathbf{Q})$, where the l-th column of $\mathbf{Q}$ contains the diagonal entries of $\mathbf{G}_2 \mathbf{R}_{xl} \mathbf{G}_2^H$. Based on the above reformulation of EIP, we can rewrite (14b) as

$$\mathbf{\Omega}^n = \arg\min_{\mathbf{\Omega}} \mathrm{Tr}\left(\mathbf{\Omega}^T \mathbf{Q}^n\right) \quad \text{s.t. } \mathbf{\Omega} \text{ is proper,} \quad (15)$$

where the l-th column of $\mathbf{Q}^n$ contains the diagonal entries of $\mathbf{G}_2 \mathbf{R}_{xl}^n \mathbf{G}_2^H$. Therefore, the EIP can be reduced by carefully choosing $\mathbf{\Omega}$. Recall that the sampling matrix $\mathbf{\Omega}$ is proper either if it is a uniformly random sampling matrix, or it has large spectral gap. However, it is difficult to incorporate such conditions in the above optimization problem.

Noticing that row and column permutation of the sampling matrix would not affect its singular values and thus the spectral gap, we propose to optimize the sampling scheme by permuting the rows and columns of an initial sampling matrix $\mathbf{\Omega}^0$, i.e.,

$$\mathbf{\Omega}^n = \arg\min_{\mathbf{\Omega}} \mathrm{Tr}\left(\mathbf{\Omega}^T \mathbf{Q}^n\right) \quad \text{s.t. } \mathbf{\Omega} \in \wp\left(\mathbf{\Omega}^0\right), \quad (16)$$

where $\wp(\mathbf{\Omega}^0)$ denotes the set of matrices obtained by arbitrary row and/or column permutations. The $\mathbf{\Omega}^0$ is generated with binary entries and $\lfloor pLM_{r,R} \rfloor$ ones. One good candidate for $\mathbf{\Omega}^0$ would be a uniformly random sampling matrix, as such matrix exhibit large spectral gap with high probability [34]. Brute-force search can be used to find the optimal $\mathbf{\Omega}$. However, the complexity is very high since $|\wp(\mathbf{\Omega}^0)| = \Theta(M_{r,R}!L!)$. By alternately optimizing w.r.t. row permutation and column permutation on $\mathbf{\Omega}^0$, we can solve (16) using a sequence of linear assignment problems [57].

To optimize w.r.t. column permutation, we need to find the best one-to-one match between the columns of $\mathbf{\Omega}^0$ and the columns of $\mathbf{Q}^n$. We construct a cost matrix $\mathbf{C}^c \in \mathbb{R}^{L \times L}$ with $[\mathbf{C}^c]_{ml} \triangleq (\mathbf{\Omega}_{\cdot m}^0)^T \mathbf{Q}_{\cdot l}^n$. The problem turns out to be a linear assignment problem with cost matrix $\mathbf{C}^c$, which can be solved in polynomial time using the Hungarian algorithm [57]. Let $\mathbf{\Omega}^c$ denote the column-permutated sampling matrix after the above step. Then, we permute the rows of $\mathbf{\Omega}^c$ to optimally match the rows of $\mathbf{Q}^n$. Similarly, we construct a cost matrix $\mathbf{C}^r \in \mathbb{R}^{M_{r,R} \times M_{r,R}}$ with $[\mathbf{C}^r]_{ml} \triangleq \mathbf{\Omega}_{m\cdot}^c (\mathbf{Q}_{l\cdot}^n)^T$. Again, the Hungarian algorithm can be used to solve the row assignment problem. The above column and row permutation steps are alternately repeated until $\mathrm{Tr}(\mathbf{\Omega}^T \mathbf{Q}^n)$ becomes smaller than a certain predefined threshold δ_1.

The complete joint-design spectrum sharing algorithm is summarized in Algorithm 2. The proposed algorithm stops when the value of EIP changes between two iterations drops below a certain threshold δ_2. It is easy to show that the objective function, i.e., EIP, is nonincreasing during the alternating iterations between (14a) and (14b), and is lower bounded by zero. According to the monotone convergence theorem [58], the alternating optimization is guaranteed to converge. The proposed joint-design spectrum sharing strategy is expected to further reduce the EIP at the MIMO-MC radar RX node compared to the cooperative methods in Section IV.A. However, $(\mathbf{P}_2)$ has higher computational complexity than $(\mathbf{P}_1)$ and $(\mathbf{P}_0)$ (see detailed complexity analysis in Section IV.C). $(\mathbf{P}_1)$ and $(\mathbf{P}_0)$ could be preferable in cases of limited computing resources.

C. Complexity

The adaptive communication transmission in the proposed spectrum sharing methods involves high complexity. A natural question would be how much would one lose by using a sub-optimal transmission approach of constant rate, i.e., $\mathbf{R}_{xl} = \cdots = \mathbf{R}_{xL} \equiv \mathbf{R}_x$, which has lower implementation complexity. In such case, the spectrum sharing problem $(\mathbf{P}_1)$ can be

Algorithm 2: Joint Design Based Spectrum Sharing Between MIMO-MC Radar and a MIMO Communication System.

Input: $\mathbf{H}, \mathbf{G}_1, \mathbf{G}_2, P_t, C, \sigma_C^2, \delta_1, \delta_2$
Initialization: $\mathbf{\Omega}^0$ is a uniformly random sampling matrix
repeat
  $\{\mathbf{R}_{xl}^n\} \leftarrow$ Solve problem (14a) using **Algorithm** 1 while fixing $\mathbf{\Omega}^{n-1}$
  $\mathbf{\Omega}^{prev} \leftarrow \mathbf{\Omega}^{n-1}$
  loop
    $\mathbf{\Omega}^c \leftarrow$ Find the best column permutation of $\mathbf{\Omega}^{prev}$ by solving the linear assignment problem with cost matrix $\mathbf{C}^c$
    $\mathbf{\Omega}^r \leftarrow$ Find the best row permutation of $\mathbf{\Omega}^c$ by solving the linear assignment problem with cost matrix $\mathbf{C}^r$
    if $|\mathrm{Tr}((\mathbf{\Omega}^r)^T \mathbf{Q}^n) - \mathrm{Tr}((\mathbf{\Omega}^{prev})^T \mathbf{Q}^n)| < \delta_1$ **then**
      Break
    end if
    $\mathbf{\Omega}^{prev} \leftarrow \mathbf{\Omega}^r$
  end loop
  $\mathbf{\Omega}^n \leftarrow \mathbf{\Omega}^r; n \leftarrow n+1$
until $|\mathrm{EIP}^n - \mathrm{EIP}^{n-1}| < \delta_2$
Output: $\{\mathbf{R}_{xl}\} = \{\mathbf{R}_{xl}^n\}, \mathbf{\Omega} = \mathbf{\Omega}^n$

reformulated as

$$(\mathbf{P}_1') \min_{\mathbf{R}_x \succeq 0} \mathrm{EIP}(\mathbf{R}_x) \quad \text{s.t.} \quad L\mathrm{Tr}(\mathbf{R}_x) \le P_t, \mathrm{C}_{\mathrm{avg}}(\mathbf{R}_x) \ge C, \tag{17}$$

where $\mathrm{EIP}(\mathbf{R}_x) \triangleq \mathrm{Tr}(\mathbf{\Delta}\mathbf{G}_2\mathbf{R}_x\mathbf{G}_2^H)$ and $\mathbf{\Delta}$ is diagonal and with each entry equal to the sum of the entries in the corresponding row of $\mathbf{\Omega}$. We can see that $(\mathbf{P}_1')$ is much easier to solve because there is only one matrix variable. However, as it will be seen in the simulations of Section VI.B, the constant rate transmission based on solving (9) is inferior to the adaptive transmission based on solving (17).

It is clear that $(\mathbf{P}_0)$ and $(\mathbf{P}_1)$ have the same computational complexity, because the objectives and the constraints are similar. If an interior-point method [55] is used directly to the problems, the complexity is polynomial (cubic or slightly higher orders) in the number of real variables in each problem. For both $(\mathbf{P}_0)$ and $(\mathbf{P}_1)$, the semidefinite matrix variables $\{\mathbf{R}_{xl}\}$ have $LM_{t,C}^2$ real scalar variables. For the sub-optimal $(\mathbf{P}_1')$, there is only one semidefinite matrix variable $\mathbf{R}_x$, which results in $M_{t,C}^2$ real scalar variables. Therefore, the computational costs of $(\mathbf{P}_0)$ and $(\mathbf{P}_1)$ are at least L^3 times of that of $(\mathbf{P}_1')$, which are prohibitive if L is large. Fortunately, when $(\mathbf{P}_0)$ and $(\mathbf{P}_1)$ are solved using Algorithm 1 based on dual decomposition, the computation complexity is greatly reduced and scales linearly with L. Furthermore, the overall computation time of $(\mathbf{P}_0)$ and $(\mathbf{P}_1)$ using dual decomposition even becomes independent of L and thus equal to that of $(\mathbf{P}_1')$ if all L sub-problems ($\mathbf{P}_1$-sub) are solved simultaneously in parallel using the same computational routine [31].

To solve $(\mathbf{P}_2)$, several iterations of solving problems in (14a) and (14b) are required. The computational complexity of (14a) is identical to that of $(\mathbf{P}_1)$, which has been considered previously. Problem (14b) is in turn solved via several iterations of linear assignment problem, whose complexity cubically scales with L. Simulations show that the numbers of both inner and outer iterations in Algorithm 2 are relative small. In summary, the computational complexity of $(\mathbf{P}_2)$ is the sum of L times of a polynomial of $M_{t,C}^2$ and $\mathcal{O}(L^3)$.

V. Mismatched Systems

In Section III, the waveform symbol duration of the radar system is assumed to match that of the communication system. In this section, we consider the mismatched case, and show that the proposed techniques presented in the previous sections can still be applied. Let $f_s^R = 1/T_R$ and f_s^C denote the radar waveform symbol rate and the communication symbol rate, respectively. Also, let the length of radar waveforms be denoted by L_R. The number of communication symbols transmitted in the duration of L_R/f_s^R is $L_C \triangleq \lceil L_R f_s^C f_s^R \rceil$. The communication average capacity and transmit power can be expressed in terms of $\{\mathbf{R}_{xl}\}_{l=1}^{L_C}$ as in Section IV. In the following, we will only focus on the effective interference to the MIMO-MC radar receiver.

If $f_s^R < f_s^C$, the interference arrived at the radar receiver will be down-sampled. Let $\mathcal{I}_1 \subset \mathbb{N}_{L_C}^+$ be the set of indices of communication symbols that are sampled by the radar in ascending order. It holds that $|\mathcal{I}_1| = L_R$. Following the derivation in previous sections, we have the following interference power expression:

$$\mathrm{EIP} = \sum_{l \in \mathcal{I}_1} \mathrm{Tr}\left(\mathbf{\Delta}_{l'}\mathbf{G}_2\mathbf{R}_{xl}\mathbf{G}_2^H\right),$$

where $l' \in \mathbb{N}_{L_R}^+$ is the index of l in ordered set $\mathcal{I}_1$. We observe that the communication symbols indexed by $\mathbb{N}_{L_C}^+ \backslash \mathcal{I}_1$, which are not sampled by the radar receiver, would introduce zero interference power to the radar system.

If $f_s^R > f_s^C$, the interference at the radar receiver will be over-sampled. One individual communication symbol will introduce interference to the radar system in $\lfloor f_s^R/f_s^C \rfloor$ consecutive symbol durations. Let $\widetilde{\mathcal{I}}_l$ be the set of radar sampling time instances during the period of the l-th communication symbol. Note that $\widetilde{\mathcal{I}}_l$ is with cardinality $\lfloor f_s^R/f_s^C \rfloor$, and the collection of sets $\widetilde{\mathcal{I}}_1, \ldots, \widetilde{\mathcal{I}}_{L_C}$ is a partition of $\mathbb{N}_{L_R}^+$. The effective interference power for both schemes of MIMO-MC radar is respectively

$$\mathrm{EIP} = \sum_{l=1}^{L_C} \mathrm{Tr}\left(\widetilde{\mathbf{\Delta}}_l\mathbf{G}_2\mathbf{R}_{xl}\mathbf{G}_2^H\right),$$

where $\widetilde{\mathbf{\Delta}}_l = \sum_{l' \in \widetilde{\mathcal{I}}_l} \mathbf{\Delta}_{l'}$. We observe that each individual communication transmit covariance matrix will be weighted by the sum of interference channels for $\lfloor f_s^R/f_s^C \rfloor$ radar symbol durations instead of one single interference channel.

We conclude that in the above mismatched cases, the EIP expressions have the same form as those in the matched case except the diagonal matrix $\mathbf{\Delta}_l$. To calculate the corresponding diagonal matrices, the communication system only needs to

know the sampling time of the radar system. Therefore, the spectrum sharing problems in such cases can still be solved using the proposed algorithms of Section IV.

VI. Numerical Results

For the simulations, we set the number of symbols to $L = 32$ and the noise variance to $\sigma_C^2 = 0.01$. The MIMO radar system consists of colocated TX and RX antennas forming half-wavelength uniform linear arrays, and transmitting Gaussian orthogonal waveforms [23]. The channel $\mathbf{H}$ is taken to have independent entries, distributed as $\mathcal{CN}(0, 1)$. The interference channels $\mathbf{G}_1$ and $\mathbf{G}_2$ are generated with independent entries, distributed as $\mathcal{CN}(0, \sigma_1^2)$ and $\mathcal{CN}(0, \sigma_2^2)$, respectively. The channels are Rayleigh fading and are consistent with a flat fading model assumption [5]–[9], [31], [32], [44], [45]. We fix $\sigma_1^2 = \sigma_2^2 = 0.01$ unless otherwise stated. The maximum communication transmit power is set to $P_t = L$ (the power is normalized w.r.t. the power of radar waveforms). The propagation path from the radar TX antennas to the radar RX antennas via the far-field target introduces a much more severe loss of power, γ^2, which is set to -30 dB in the simulations. The transmit power of the radar antennas is fixed to $\rho^2 = \rho_0 \triangleq 1000L/M_{t,R}$ unless otherwise stated, and noise in the received signal is added at $\mathrm{SNR} = 25$ dB. The phase jitter variance is taken to be $\sigma_\alpha^2 = 10^{-3}$. The same uniformly random sampling scheme $\mathbf{\Omega}^0$ is adopted by the radar in both the cooperative spectrum sharing (SS) methods of $(\mathbf{P}_0)$ and $(\mathbf{P}_1)$. The joint-design spectrum sharing method uses the same sampling matrix as its initial sampling matrix. Recall that $(\mathbf{P}_0)$ is the cooperative spectrum sharing method when $\mathbf{\Omega}$ is not shared with the communication system. In $(\mathbf{P}_0)$, the communication system designs its waveforms by assuming $\mathbf{\Omega}$ as the all 1's matrix. Based on the obtained communication waveforms, an EIP value is calculated for $(\mathbf{P}_0)$ using the true $\mathbf{\Omega}$ for the ease of comparison. In the following figures, we denote the cooperative spectrum sharing method of $(\mathbf{P}_0)$ without knowledge of $\mathbf{\Omega}$ by "cooperative SS w/ $\mathbf{\Omega}$ unknown". We denote the cooperative spectrum sharing method of $(\mathbf{P}_1)$ by "cooperative SS"; and denote the joint-design spectrum sharing method of $(\mathbf{P}_2)$ by "joint-design SS". The TFOCUS package [59] is used for low-rank matrix completion at the radar fusion center. The communication covariance matrix is optimized according to the criteria of Section IV. The obtained $\mathbf{R}_{xl}$ is used to generate $\mathbf{x}(l) = \mathbf{R}_{xl}^{1/2}\mathrm{randn}(M_{t,C}, 1)$. We use the EIP and MC relative recovery error as the performance metrics. The relative recovery error is defined as $\| \mathbf{DS} - \widehat{\mathbf{DS}}\|_F / \| \mathbf{DS} \|_F$, where $\widehat{\mathbf{DS}}$ is the completed result of $\mathbf{DS}$. For comparison, we also implement a "selfish communication" scenario, where the communication system minimizes the transmit power to achieve certain average capacity without any concern about the interferences it exerts to the radar system.

A. The Impact of EIP on Matrix Completion and Target Angle Estimation

In the following we provide simulation results in support of the use of EIP as a design objective. We take $M_{t,R} = 16, M_{r,R} = 32, M_{t,C} = 4, M_{r,C} = 4$. We consider two far-field targets at angle 30° and 32.5° w.r.t. the radar arrays, with target reflection coefficients equal to $0.2 + 0.1j$. The sub-sampling rate of MIMO-MC radar is fixed to 0.5. We simulate different levels of EIP by setting the communication TX covariance matrices equal to identity matrix and varying a scaling parameter. In Fig. 2, we show the MC relative recovery errors and target angle estimation success rates under different levels of EIP. The angle estimation is achieved by the MUSIC method based on 5 pulses [24]. A success occurs if the angle estimation error is smaller than 0.25°. The results are calculated based on 200 independent trials. One can see that the EIP indeed greatly affects the matrix completion accuracy and further the target angle estimation. In particular, a 0.5 unit increase of EIP causes a sharp 30% drop of the target angle estimation success rate. Therefore, in order to guarantee the function of the MIMO-MC radar, the EIP has to be maintained at a small level.

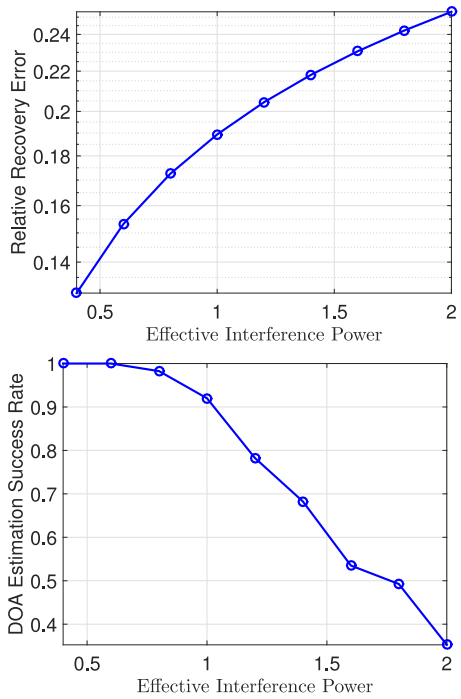

Fig. 2. MC relative recovery and target angle estimation success rate under different levels of EIP for the MIMO-MC radar. $M_{t,R} = 16, M_{r,R} = 32, M_{t,C} = 4, M_{r,C} = 4$.

B. Spectrum Sharing Based on Adaptive Transmission and Constant Rate Transmission

In this simulation, we compare the performance of the cooperative scheme of $(\mathbf{P}_1)$ based on adaptive transmission and the constant rate transmission scheme of $(\mathbf{P}_1')$. We also implement the selfish communication scenario using constant rate transmission. We take $M_{t,R} = 4, M_{r,R} = M_{t,C} = 8, M_{r,C} = 4$, and one far-field stationary target at angle 30° w.r.t. the radar arrays, with target reflection coefficient equal to $0.2 + 0.1j$. For the communication capacity constraint, we consider $C = 12$ bits/symbol. Fig. 3 shows the EIP and MC relative recovery error as functions of the sub-sampling rate at the MIMO-MC radar. We observe that the cooperative scheme of $(\mathbf{P}_1)$ (labeled as "Cooperative SS + Adaptive") achieves much smaller EIP and

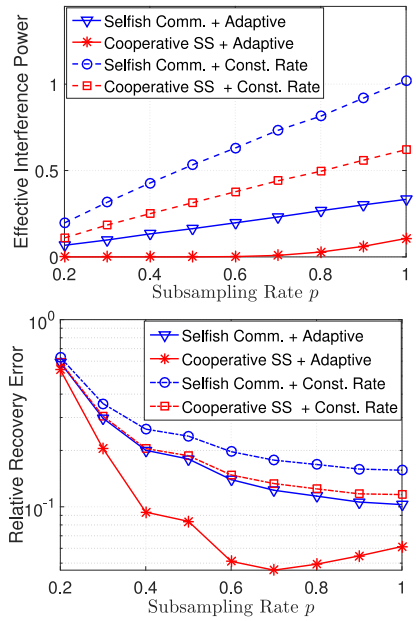

Fig. 3. Spectrum sharing based on adaptive transmission and constant rate transmission for the MIMO-MC radar. $M_{t,R} = 4, M_{r,R} = M_{t,C} = 8, M_{r,C} = 4$.

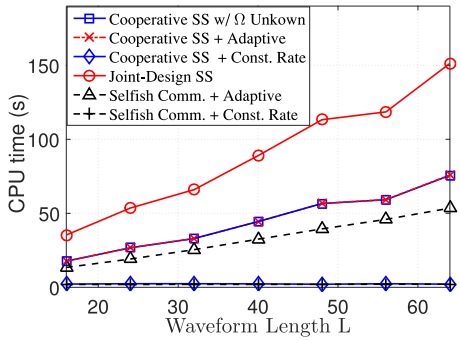

Fig. 4. CPU time comparison for various spectrum sharing algorithms under different values of waveform length L.

MC errors than the constant rate transmission scheme of $(\mathbf{P}_1')$ (labeled as "Cooperative SS + Const. Rate") does. It can also be seen that the constant rate transmission scheme is inferior even to the adaptive transmission based selfish communication scheme. This implies that the adaptive transmission technique plays an important role in reducing the EIP and MC errors. In the following, the performance of adaptive transmission based schemes is evaluated in more detail. As we already mentioned in Section II, when the sub-sampling rate p equals 1, the MIMO-MC radar becomes the traditional MIMO radar. Therefore, the above comparison between the adaptive and the constant rate transmission scheme for MIMO-MC radars also holds for traditional MIMO radars.

To get an idea of the complexity involved in the aforementioned simulations, we recorded the CPU times for the various spectrum sharing algorithms executed on a laptop with Intel Core i7 CPU and 8 GB memory. Fig. 4 shows the CPU times under different values of waveform length. One can observe that 1) the constant rate algorithms are the fastest and their running

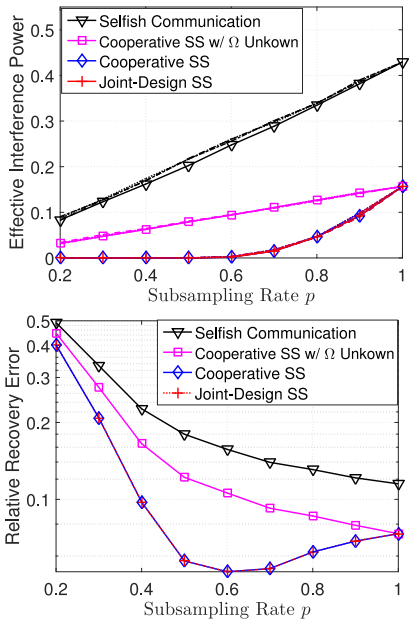

Fig. 5. Spectrum sharing with the MIMO-MC radar under different sub-sampling rates. $M_{t,R} = 4, M_{r,R} = M_{t,C} = 8, M_{r,C} = 4$. Dashed curves correspond to EIP results using different realization of $\mathbf{\Omega}^0$.

times are independent of L; 2) the running times of the adaptive rate algorithms, both selfish and cooperative ones, scale linearly with L; 3) the joint-design spectrum sharing method takes about 2–3 times of the cooperative spectrum sharing methods' running time. These observations match our complexity analysis in Section IV.C.

C. *Spectrum Sharing Between a MIMO-MC Radar and a MIMO Communication System*

1) Performance Under Different Sub-Sampling Rates: There is a far-field stationary target at angle 30° w.r.t. the radar arrays, with target reflection coefficient equal to $0.2 + 0.1j$. For the communication capacity constraint, we consider $C = 12$ bits/symbol. The sub-sampling rate of MIMO-MC radar varies from 0.2 to 1. The following two scenarios are considered.

In the first scenario, we take $M_{t,R} = 4, M_{r,R} = M_{t,C} = 8, M_{r,C} = 4$. In Fig. 5(a) we plot the EIP results for 4 different realizations of $\mathbf{\Omega}^0$. For better visualization, Fig. 5(b) shows the relative recovery errors averaged over all 4 realizations of $\mathbf{\Omega}^0$. The cooperative scheme (see $\mathbf{P}_1$) outperforms its counterpart without knowledge of $\mathbf{\Omega}$ (see $\mathbf{P}_0$) in terms of both the EIP and the MC relative recovery error. As discussed in Section IV, the EIP is significantly reduced by the cooperative method when $p < 0.6$, i.e., when $pM_{r,R}$ is much smaller than $M_{t,C}$. The joint-design scheme in this scenario performs the same as the cooperative scheme, possibly because the row dimension of $\mathbf{\Omega}$ is too small to generate sufficient difference in EIP among the various permutations of $\mathbf{\Omega}$.

In the second scenario, we take $M_{t,R} = 16, M_{r,R} = 32, M_{t,C} = 4, M_{r,C} = 4$. In Fig. 6(a), we plot the EIP corresponding to 4 different realizations of $\mathbf{\Omega}^0$, taken as uniformly random sampling matrices. Again, Fig. 6(b) shows the relative

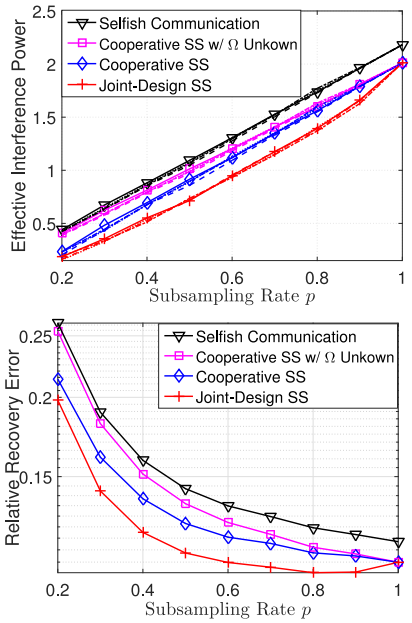

Fig. 6. Spectrum sharing with the MIMO-MC radar under different sub-sampling rates. $M_{t,R} = 16, M_{r,R} = 32, M_{t,C} = M_{r,C} = 4$. Dashed curves correspond to EIP results using different realization of $\mathbf{\Omega}^0$.

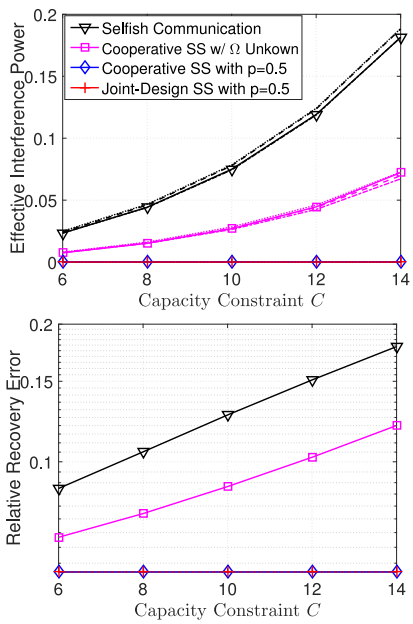

Fig. 7. Spectrum sharing with the MIMO-MC radar under different capacity constraints C. $M_{t,R} = 4, M_{r,R} = M_{t,C} = 8, M_{r,C} = 4$. Dashed curves correspond to EIP results using different realization of $\mathbf{\Omega}^0$.

recovery errors averaged over all 4 realizations of $\mathbf{\Omega}^0$. The cooperative scheme outperforms the cooperative scheme without knowledge of $\mathbf{\Omega}$ only marginally. This is due to the fact that both $\mathbf{G}_2$ and $\mathbf{G}_{2l}$ are full rank. The joint-design scheme (see Section IV.B) optimizes $\mathbf{\Omega}$ starting from the same sampling matrix used by the other three methods. In this case, the joint-design scheme achieves smaller EIP and relative recovery errors than the other three methods.

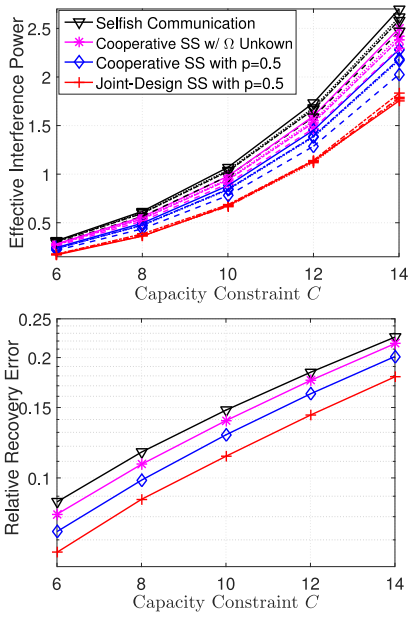

Fig. 8. Spectrum sharing with the MIMO-MC radar under different capacity constraints C. $M_{t,R} = 16, M_{r,R} = 32, M_{t,C} = M_{r,C} = 4$. Dashed curves correspond to EIP results using different realization of $\mathbf{\Omega}^0$.

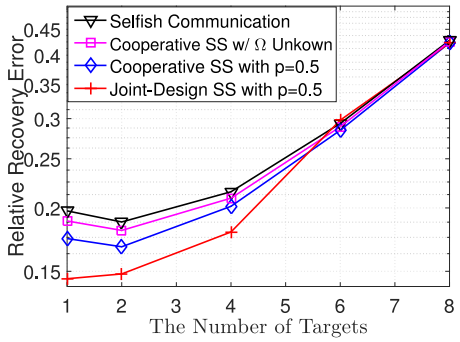

Fig. 9. Spectrum sharing with the MIMO-MC radar when multiple targets present. $M_{t,R} = 16, M_{r,R} = 32, M_{t,C} = M_{r,C} = 4p = 0.5$ and $C = 12$ bits/symbol.

In the above scenarios, we would like $p \geq 0.5$ for a small relative recovery error during matrix completion. However, values of $p > 0.7$ require more samples while achieving little or even no improvement on the recovery accuracy. Therefore, the optimal range of p is [0.5, 0.7], where the proposed joint-design scheme significantly outperforms the "selfish communication method" and the "SS method w/o knowledge of $\mathbf{\Omega}$". We conclude that the proposed co-design based spectrum sharing methods utilize the sub-sampling procedure in the MIMO-MC radar to achieve small EIP and high matrix recovery accuracy.

Interestingly, for the joint-design based spectrum sharing method, the relative recovery error achieved by the sub-sampling rate $p \in [0.5, 0.9]$ is even smaller than that by full samp ling $p = 1$. This indicates that due to the achieved small EIP, the full signal matrix is accurately completed. The completion process smooths out the noise, and as result, the completed matrix enjoys higher SIR that the initial full signal matrix. Therefore, the sub-sampling procedure in MIMO-MC radar is beneficial

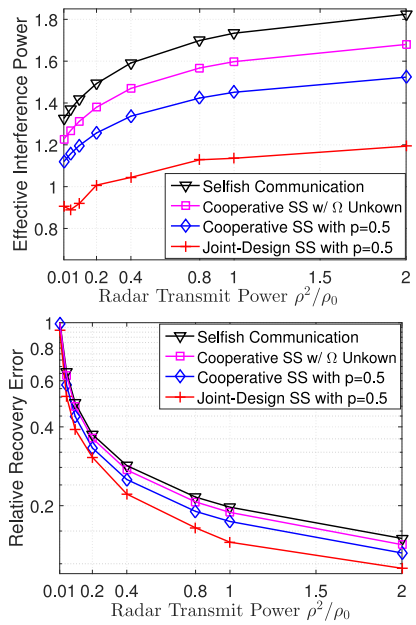

Fig. 10. Spectrum sharing with the MIMO-MC radar under different levels of radar TX power. $M_{t,R} = 16, M_{r,R} = 32, M_{t,C} = M_{r,C} = 4$.

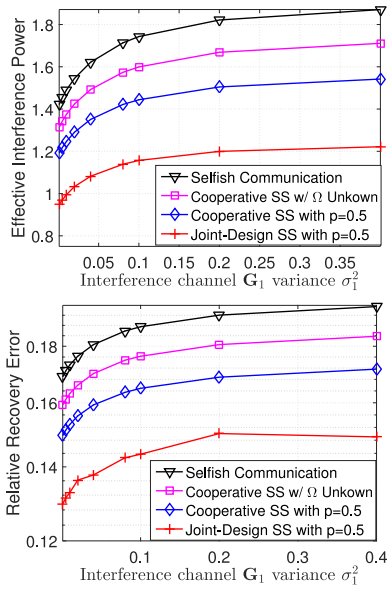

Fig. 11. Spectrum sharing with the MIMO-MC radar under different channel variance σ_1^2 for the interference channel $\mathbf{G}_1$. $M_{t,R} = 16, M_{r,R} = 32, M_{t,C} = M_{r,C} = 4$.

for radar-communication spectrum sharing in terms of improving radar SINR as well as reducing the amount of data to be sent to the fusion center.

In addition, simulations indicate that the communication average capacity constraint holds with equality in both scenarios, confirming observation (1) of Section IV.A.

2) Performance Under Different Capacity Constraints: In this simulation, the constant C in the communication capacity constraint of (9b) varies from 6 to 14 bits/symbol, while the sub-sampling rate p is fixed to 0.5. Four different realizations of Ω^0 are considered. Fig. 7 shows the results for $M_{t,R} = 4, M_{r,R} = M_{t,C} = 8, M_{r,C} = 4$. For the "selfish communication" scheme and the cooperative scheme without knowledge of $\mathbf{\Omega}$, the EIP and relative recovery errors increase as the communication capacity increases. In contrast, the cooperative and joint-design schemes achieve significantly smaller EIP and relative recovery errors under all values of C. This indicates that the latter two spectrum sharing methods successfully allocate the communication transmit power in directions that result in high communication rate, but small EIP to the MIMO-MC radar.

The results for $M_{t,R} = 16, M_{r,R} = 32, M_{t,C} = M_{r,C} = 4$ are shown in Fig. 8. Since $M_{r,R}$ is much larger than $M_{t,C}$, the cooperative scheme with the knowledge of $\mathbf{\Omega}$ outperforms its counterpart without knowledge of $\mathbf{\Omega}$ only marginally. Meanwhile, the joint-design scheme can effectively further reduce the EIP and relative recovery errors.

3) Performance Under Different Number of Targets: In this simulation, we fix $p = 0.5$ and $C = 12$ and evaluate the performance when multiple targets are present. The target reflection coefficients are designed such that the target returns have fixed power, independent of the number of targets. We observe that the EIPs of different methods remain constant for different number of targets. This is because the design of the communication waveforms is not affected by the target number. Fig. 9 shows the results of the relative recovery error, which increases as the number of targets increases. All methods have large recovery error for large number of targets, because the retained samples are not sufficient for reliable matrix completion under any level of noise. The proposed joint-design scheme can work effectively for the MIMO-MC radar when a moderate number of targets are present.

4) Performance Under Different Levels of Radar TX Power: In this simulation, we evaluate the effect of radar TX power ρ_2, while fixing $p = 0.5$, $C = 12$ and the target number to be 1. Fig. 10 shows the results of EIP and relative recovery errors for $M_{t,R} = 16, M_{r,R} = 32, M_{t,C} = M_{r,C} = 4$. Again, we see that the joint-design scheme performs the best, followed by the cooperative scheme with the knowledge of $\mathbf{\Omega}$ and then the cooperative scheme without knowledge of $\mathbf{\Omega}$. When the radar TX power increases, the EIP increases but with a much slower rate. Therefore, increasing the radar TX power improves the relative recovery errors.

5) Performance Under Different Interference Channel Strength: In this simulation, we evaluate the effect the interference channel $\mathbf{G}_1$ with different σ_1^2, while fixing $p = 0.5$, $C = 12$ and the target number to be 1. As the communication RX gets closer to the radar TX antennas, σ_1^2 gets larger. Fig. 11 shows the results of EIP and relative recovery errors for $M_{t,R} = 16, M_{r,R} = 32, M_{t,C} = M_{r,C} = 4$. For all the spectrum sharing methods, when the interference channel $\mathbf{G}_1$ gets stronger, the communication TX increases its transmit power in order to satisfy the capacity constraint. Therefore, the EIP and the relative recovery errors increases with the variance σ_1^2. We also observe that the joint-design scheme performs the best, followed by the cooperative scheme with the knowledge of $\mathbf{\Omega}$ and then the cooperative scheme without knowledge of $\mathbf{\Omega}$.

VII. Conclusion

This paper has considered spectrum sharing between a MIMO communication system and a MIMO-MC radar system. In order to reduce the effective interference power (EIP) at radar RX antennas, we have first considered the cooperative spectrum sharing method, which designs the communication transmit covariance matrix based on the knowledge of the radar sampling scheme. We have also formulated the spectrum sharing method for the case where the radar sampling scheme is not shared with the communication system. Our theoretical results guarantee that the cooperative approach can effectively reduce the EIP to a larger extent as compared to the spectrum sharing method without the knowledge of the radar sampling scheme. Second, we have proposed a joint design of the communication transmit covariance matrix and the radar sampling scheme to further reduce the EIP. The EIP reduction and the matrix completion recovery errors have been evaluated under various system parameters. We have shown that the MIMO-MC radars enjoy reduced interference by the communication system when the proposed spectrum sharing methods are considered. In particular, the sparse sampling at the radar RX antennas can reduce the rank of the interference channel. Our simulations have confirmed that significant EIP reduction is achieved by the cooperative approach; this is because in that approach, the communication power is allocated to directions in the null space of the effective interference channel. Our simulations have suggested that the joint-design scheme can achieve much smaller EIP and relative recovery errors than other methods when the number of radar TX and RX antennas is moderately large.

The adaptive communication transmission has been shown to be the optimal scheme for the considered spectrum sharing scenario. Compared to the constant rate transmission, the adaptive transmission requires higher computational and implementation complexity. To reduce the computation complexity, efficient algorithms have been provided based on the Lagrangian dual decomposition. As more and more powerful digital signal processors are used in modern communication terminals, advanced adaptive transmission approaches ought to weigh heavily due to the increasing demand on high spectral efficiency. Nevertheless, the adaptive transmission approach considered in the paper provides useful insights on the optimal design of the MIMO communication system coexisting with MIMO-MC radars, which deserves research attention despite the computational and implementation complexity.

References

[1] B. Li and A. P. Petropulu, "Spectrum sharing between matrix completion based MIMO radars and a MIMO communication system," in *Proc. IEEE Int. Conf. Acoust., Speech, Signal Process.*, Apr. 2015, pp. 2444–2448.

[2] Radar Spectrum Regulatory Overview, 2013, [Online]. Available: http://www.darpa.mil/WorkArea/DownloadAsset.aspx?id=2147486331

[3] F. H. Sanders, R. L. Sole, J. E. Carroll, G. S. Secrest, and T. L. Allmon, "Analysis and resolution of RF interference to radars operating in the band 2700–2900 MHz from broadband communication transmitters," U.S. Dept. of Commerce, Tech. Rep. Tech. Rep. NTIA Tech. Rep. TR-13-490, 2012.

[4] A. Lackpour, M. Luddy, and J. Winters, "Overview of interference mitigation techniques between WiMAX networks and ground based radar," in *Proc. 20th Annu. Wireless Opt. Commun. Conf.*, Apr. 2011, pp. 1–5.

[5] S. Sodagari, A. Khawar, T. C. Clancy, and R. McGwier, "A projection based approach for radar and telecommunication systems coexistence," in *Proc. IEEE Global Telecommun. Conf.*, Dec. 2012, pp. 5010–5014.

[6] A. Babaei, W. H. Tranter, and T. Bose, "A practical precoding approach for radar/communications spectrum sharing," in *Proc. 8th Int. Conf. Cognit. Radio Orient. Wireless Netw.*, Jul. 2013, pp. 13–18.

[7] S. Amuru, R. M. Buehrer, R. Tandon, and S. Sodagari, "MIMO radar waveform design to support spectrum sharing," in *Proc. IEEE Military Commun. Conf.*, Nov. 2013, pp. 1535–1540.

[8] A. Khawar, A. Abdel-Hadi, and T. C. Clancy, "Spectrum sharing between S-band radar and LTE cellular system: A spatial approach," in *Proc. IEEE Int. Symp. Dynam. Spectrum Access Netw.*, Apr. 2014, pp. 7–14.

[9] C. Shahriar, A. Abdelhadi, and T. C. Clancy, "Overlapped-MIMO radar waveform design for coexistence with communication systems," in *Proc. IEEE Wireless Commun. Netw. Conf.*, 2015, pp. 223–228.

[10] H. Deng and B. Himed, "Interference mitigation processing for spectrum-sharing between radar and wireless communications systems," *IEEE Trans. Aerosp. Electron. Syst.*, vol. 49, no. 3, pp. 1911–1919, Jul. 2013.

[11] A. Aubry, A. De Maio, M. Piezzo, and A. Farina, "Radar waveform design in a spectrally crowded environment via nonconvex quadratic optimization," *IEEE Trans. Aerosp. Electron. Syst.*, vol. 50, no. 2, pp. 1138–1152, 2014.

[12] A. Aubry, A. De Maio, Y. Huang, M. Piezzo, and A. Farina, "A new radar waveform design algorithm with improved feasibility for spectral coexistence," *IEEE Trans. Aerosp. Electron. Syst.*, vol. 51, no. 2, pp. 1029–1038, Apr. 2015.

[13] S. C. Surender, R. M. Narayanan, and C. R. Das, "Performance analysis of communications & radar coexistence in a covert UWB OSA system," in *Proc. IEEE Global Telecommun. Conf.*, 2010, pp. 1–5.

[14] A. Turlapaty and Y. Jin, "A joint design of transmit waveforms for radar and communications systems in coexistence," in *Proc. IEEE Radar Conf.*, 2014, pp. 0315–0319.

[15] E. Fishler, A. Haimovich, R. Blum, D. Chizhik, L. Cimini, and R. Valenzuela, "MIMO radar: An idea whose time has come," in *Proc. IEEE Radar Conf.*, Apr. 2004, pp. 71–78.

[16] J. Li and P. Stoica, "MIMO radar with colocated antennas," *IEEE Signal Process. Mag.*, vol. 24, no. 5, pp. 106–114, 2007.

[17] J. Li, P. Stoica, L. Xu, and W. Roberts, "On parameter identifiability of MIMO radar," *IEEE Signal Process. Lett.*, vol. 14, no. 12, pp. 968–971, Dec. 2007.

[18] C. Chen and P. P. Vaidyanathan, "MIMO radar space time adaptive processing using prolate spheroidal wave functions," *IEEE Trans. Signal Process.*, vol. 56, no. 2, pp. 623–635, Feb. 2008.

[19] C. Chen and P. P. Vaidyanathan, "MIMO radar ambiguity properties and optimization using frequency-hopping waveforms," *IEEE Trans. Signal Process.*, vol. 56, no. 12, pp. 5926–5936, 2008.

[20] M. A. Herman and T. Strohmer, "High-resolution radar via compressed sensing," *IEEE Trans. Signal Process.*, vol. 57, no. 6, pp. 2275–2284, Jun. 2009.

[21] Y. Yu, A. P. Petropulu, and H. V. Poor, "MIMO radar using compressive sampling," *IEEE J. Sel. Topics Signal Process.*, vol. 4, no. 1, pp. 146–163, Feb. 2010.

[22] M. Rossi, A. M. Haimovich, and Y. C. Eldar, "Spatial compressive sensing for MIMO radar," *IEEE Trans. Signal Process.*, vol. 62, no. 2, pp. 419–430, Jan. 2014.

[23] S. Sun, A. P. Petropulu, and W. U. Bajwa, "Target estimation in colocated MIMO radar via matrix completion," in *Proc. IEEE Int. Conf. Acoust., Speech, Signal Process.*, May 2013, pp. 4144–4148.

[24] S. Sun, W. Bajwa, and A. P. Petropulu, "MIMO-MC radar: A MIMO radar approach based on matrix completion," *IEEE Trans. Aerosp. Electron. Syst.*, vol. 51, no. 3, pp. 1839–1852, Jul. 2015.

[25] D. S. Kalogerias and A. P. Petropulu, "Matrix completion in colocated MIMO radar: Recoverability, bounds and theoretical guarantees," *IEEE Trans. Signal Process.*, vol. 62, no. 2, pp. 309–321, Jan. 2014.

[26] S. Sun and A. P. Petropulu, "Waveform design for MIMO radars with matrix completion," *IEEE J. Sel. Topics Signal Process.*, vol. 9, no. 8, pp. 1400–1414, Dec. 2015.

[27] Y. Chi, L. L. Scharf, A. Pezeshki, and A. R. Calderbank, "Sensitivity to basis mismatch in compressed sensing," *IEEE Trans. Signal Process.*, vol. 59, no. 5, pp. 2182–2195, May 2011.

[28] B. Li and A. P. Petropulu, "Radar precoding for spectrum sharing between matrix completion based MIMO radars and a MIMO communication system," in *Proc. IEEE Global Conf. Signal Inf. Process.*, Dec. 2015, pp. 737–741.

[29] K. Letaief and W. Zhang, "Cooperative communications for cognitive radio networks," *Proc. IEEE*, vol. 97, no. 5, pp. 878–893, May 2009.
[30] S. Haykin, "Cognitive radar: A way of the future," *IEEE Signal Process. Mag.*, vol. 23, no. 1, pp. 30–40, Jan. 2006.
[31] R. Zhang and Y. Liang, "Exploiting multi-antennas for opportunistic spectrum sharing in cognitive radio networks," *IEEE J. Sel. Topics Signal Process.*, vol. 2, no. 1, pp. 88–102, Feb. 2008.
[32] R. Zhang, Y. Liang, and S. Cui, "Dynamic resource allocation in cognitive radio networks," *IEEE Signal Process. Mag.*, vol. 27, no. 3, pp. 102–114, May 2010.
[33] S. J. Kim and G. B. Giannakis, "Optimal resource allocation for MIMO Ad Hoc cognitive radio networks," *IEEE Trans.Inf. Theory*, vol. 57, no. 5, pp. 3117–3131, May 2011.
[34] S. Bhojanapalli and P. Jain, "Universal matrix completion," in *Proc. 31st Int. Conf. Mach. Learn.*, 2014, pp. 1881–1889.
[35] H. Krim and M. Viberg, "Two decades of array signal processing research: The parametric approach," *IEEE Signal Process. Mag.*, vol. 13, no. 4, pp. 67–94, 1996.
[36] E. J. Candes and Y. Plan, "Matrix completion with noise," *Proc. IEEE*, vol. 98, no. 6, pp. 925–936, Jun. 2010.
[37] F. M. Gardner, *Phaselock Techniques*. New York, NY, USA: Wiley, 2005.
[38] R. Poore, "Overview on phase noise and jitter," Keysight Technologies, Santa Rosa, CA, USA, Tech. Overview, 2014. [Online]. Available: http://literature.cdn.keysight.com/litweb/pdf/5990-3108EN.pdf?id=827513
[39] R. Mudumbai, G. Barriac, and U. Madhow, "On the feasibility of distributed beamforming in wireless networks," *IEEE Trans. Wireless Commun.*, vol. 6, no. 5, pp. 1754–1763, 2007.
[40] B. Razavi, "A study of phase noise in CMOS oscillators," *IEEE J. Solid-State Circuits*, vol. 31, no. 3, pp. 331–343, 1996.
[41] C. Kopp, "Search and acquisition radars (S-band, X-band)," Tech. Rep. Tech. Rep. APA-TR-2009-0101, 2009. [Online]. Available: http://www.ausairpower.net/APA-Acquisition-GCI.html
[42] Radar Performance, Radtec Engineering Inc., 2015. [Online]. Available: http://www.radar-sales.com/PDFs/Performance_RDR%26TDR.pdf
[43] "LTE in a nutshell: The physical layer," (White paper), Telesystem Innovations, Markham, ON, Canada, 2010. [Online]. Available: https://www.scribd.com/doc/297688375/LTE-in-a-Nutshell-Physical-Layer
[44] T. S. Rappaport *et al.*, *Wireless Communications: Principles and Practice*. Englewood Cliffs, NJ, USA: Prentice-Hall PTR, 2001, vol. 2.
[45] D. Tse and P. Viswanath, *Fundamentals of Wireless Communication*. Cambridge, U.K.: Cambridge Univ. Press, 2005.
[46] A. Goldsmith, *Wireless Communications*. Cambridge, U.K.: Cambridge Univ. Press, 2005.
[47] R. P. Jover, LTE PHY Fundamentals, 2015. [Online]. Available: http://www.ee.columbia.edu/roger/LTE_PHY_fundamentals.pdf
[48] M. Filo, A. Hossain, A. R. Biswas, and R. Piesiewicz, "Cognitive pilot channel: Enabler for radio systems coexistence," in *Proc. 2nd Int. Workshop Cognit. Radio Adv. Spectrum Manag.*, May 2009, pp. 17–23.
[49] L. Lu, X. Zhou, U. Onunkwo, and G. Y. Li, "Ten years of research in spectrum sensing and sharing in cognitive radio.," *EURASIP J. Wireless Commun Netw.*, vol. 2012, p. 28, 2012.
[50] G. Taubock, "Complex-valued random vectors and channels: Entropy, divergence, and capacity," *IEEE Trans. Inf. Theory*, vol. 58, no. 5, pp. 2729–2744, 2012.
[51] S. N. Diggavi and T. M. Cover, "The worst additive noise under a covariance constraint," *IEEE Trans. Inf. Theory*, vol. 47, no. 7, pp. 3072–3081, Nov. 2001.
[52] C. Chen and P. P. Vaidyanathan, "MIMO radar waveform optimization with prior information of the extended target and clutter," *IEEE Trans. Signal Process.*, vol. 57, no. 9, pp. 3533–3544, 2009.
[53] G. Cui, H. Li, and M. Rangaswamy, "MIMO radar waveform design with constant modulus and similarity constraints," *IEEE Trans. Signal Process.*, vol. 62, no. 2, pp. 343–353, 2014.
[54] A. Goldsmith, S. A. Jafar, N. Jindal, and S. Vishwanath, "Capacity limits of MIMO channels," *IEEE J. Sel. Areas Commun.*, vol. 21, no. 5, pp. 684–702, 2003.
[55] S. Boyd and L. Vandenberghe, *Convex Optimization*. Cambridge, U.K.: Cambridge Univ. Press, 2004.
[56] R. G. Bland, D. Goldfarb, and M. J. Todd, "The ellipsoid method: A survey," *Oper. Res.*, vol. 29, no. 6, pp. 1039–1091, 1981.
[57] H. W. Kuhn, "The Hungarian method for the assignment problem," *Naval Res. Logist. Quart.*, vol. 2, no. 1–2, pp. 83–97, 1955.
[58] J. Yeh, "Real analysis," *Theory of Measure and Integration*. Singapore: World Scientific, 2006.
[59] S. R. Becker, E. J. Candès, and M. C. Grant, "Templates for convex cone problems with applications to sparse signal recovery," *Math. Programm. Comput.*, vol. 3, no. 3, pp. 165–218, 2011.

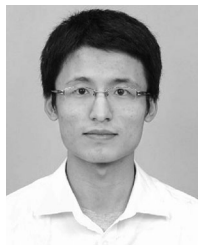

Bo Li (S'13) received his B.E. degree in communication engineering from Lanzhou University, China, in 2009, and the M.S. degree in electrical engineering from Peking University, China, in 2012. Since September 2012, he has been working towards the Ph.D. degree at the Department of Electrical & Computer Engineering, Rutgers, The State University of New Jersey, and he is a member of the Signal Processing and Communications Laboratory (CSPL). His research interests are in signal processing for MIMO radar and communication systems, including compressive sensing and matrix completion based MIMO radar, spectrum sharing in cooperative radar, and communication systems.

Athina P. Petropulu (F'08) received her undergraduate degree from the National Technical University of Athens, Greece, and the M.Sc. and Ph.D. degrees from Northeastern University, Boston MA, all in electrical and computer engineering. Since 2010, she is Professor of the Electrical and Computer Engineering (ECE) Department at Rutgers, having served as chair of the department during 2010–2016. Before that she was faculty at Drexel University. Dr. Petropulu's research interests span the area of statistical signal processing, wireless communications, signal processing in networking, physical layer security, and radar signal processing. Her research has been funded by various government industry sponsors including the National Science Foundation, the Office of Naval research, the U.S. Army, the National Institute of Health, the Whitaker Foundation, Lockheed Martin.

Dr. Petropulu is recipient of the 1995 Presidential Faculty Fellow Award given by NSF and the White House. She has served as Editor-in-Chief of the IEEE TRANSACTIONS ON SIGNAL PROCESSING (2009–2011), IEEE Signal Processing Society Vice President—Conferences (2006–2008), and member-at-large of the IEEE Signal Processing Board of Governors. She was the General Chair of the 2005 International Conference on Acoustics Speech and Signal Processing (ICASSP-05), Philadelphia PA. In 2005 she received the *IEEE Signal Processing Magazine* Best Paper Award, and in 2012 the IEEE Signal Processing Society Meritorious Service Award. More information on her work can be found at www.ece.rutgers.edu/∼cspl

Wade Trappe (F'14) is a Professor with the Department of Electrical and Computer Engineering, Rutgers University, New Brunswick, NJ, USA, and an Associate Director of the Wireless Information Network Laboratory (WINLAB), where he directs WINLABs research in wireless security. He has led several federally funded projects in the area of cybersecurity and communication systems, projects involving security and privacy for sensor networks, physical layer security for wireless systems, a security framework for cognitive radios, the development of wireless testbed resources (the ORBIT testbed), and new RFID technologies. His experience in network security and wireless spans over 15 years, and he has coauthored a popular textbook in security, Introduction to Cryptography with Coding Theory, as well as several monographs on wireless security, including *Securing Wireless Communications at the Physical Layer and Securing Emerging Wireless Systems: Lower-layer Approaches*. He served as an Editor for the IEEE TRANSACTIONS ON INFORMATION FORENSICS AND SECURITY (TIFS), the *IEEE Signal Processing Magazine* (SPM), and the IEEE TRANSACTIONS ON MOBILE COMPUTING (TMC). He served as the Lead Guest Editor for September 2011 IEEE TRANSACTIONS ON INFORMATION FORENSICS AND SECURITY Special Issue on Using the Physical Layer for Securing the Next Generation of Communication Systems and served as the IEEE Signal Processing Society representative to the governing board of IEEE TMC. He is currently the IEEE SPS Regional Director for Regions 1–6.